

Metal Switch for Amyloid Formation: Insight into the Structure of the Nucleus

David M. Morgan,[†] Jijun Dong,[†] Jaby Jacob,^{‡,||} Kun Lu,[†] Robert P. Apkarian,[†] Pappannan Thiyagarajan,^{*,‡} and David G. Lynn^{*,†}

Center for the Analysis of SupraMolecular Self-assemblies, Departments of Chemistry and Biology, Emory University, 1521 Pierce Drive, Atlanta, Georgia 30322, Biochemistry and Molecular Biology, University of Chicago, Chicago, Illinois 60637, and Intense Pulsed Neutron Source, Argonne National Laboratory, Argonne, Illinois 60439

Received June 16, 2002

Although the precise mechanism of amyloid fibril formation remains obscure,^{1–3} the self-assembly process is generally observed to follow nucleation-dependent growth *in vitro*.^{4–7} With an experimentally constrained model for the structure of the A β (10–35) fibrils,^{8–12} the central fragment of the A β peptide of Alzheimer's disease (AD), it becomes possible to better predict features that might be present in the nucleus. Here we describe conditions that radically alter the relative rates of nucleation and propagation in amyloid formation and discuss these findings in terms of their implications for the structure of the nucleus.

The fibrils formed by A β (10–35) peptides consist of strands aggregated in parallel in register β -sheets, with a spacing of 5 Å between strands within a sheet (Figure 1a). Six such sheets are laminated together, spaced by 10 Å, to give a rectangular fibril. In this structure, the side chains of the histidine residues at positions 13 and 14 are directed to opposite surfaces of the β sheet, and spaced 5 Å apart along the sheet (Figure 1b). If the sheets within the fibril were themselves parallel, as has been suggested by enzymatic cross-linking experiments,¹¹ H13 and H14 residues from different sheets would be proximal (Figure 1c). Both arrangements provide potential chelating Zn²⁺ binding sites, either along or between the sheets or, in combination, a tetravalent site.

While the histidine residues at positions 6, 13, and 14 of full length β -amyloid A β (1–42) have been implicated in metal binding, 13 and 14 appear to be most critical.^{13,14} To emphasize the impact of these interactions on fibril formation, a shortened variant, YEVHHQKLVFFA, was synthesized via standard Fmoc solid-phase chemistry to give the previously unreported A β (10–21). This peptide maintains the overall amphiphilic distribution of amino acids, polar N-terminal and nonpolar C-terminal residues that exists in A β (1–42), found to be critical for the self-assembly of A β (10–35).⁹ As was found with the longer variants, fibrils formed with A β (10–21) exhibited the green birefringence characteristic of amyloid stained with Congo Red when viewed with polarized light, and the red shift in the absorption spectrum of Congo Red from 495 nm to 515 nm, indicating that A β (10–21) indeed formed amyloid.¹⁵

A measure of the rate of fibril formation is obtained by plotting the intensity of small angle neutron scattering (SANS) at $Q = 0.03 \text{ \AA}^{-1}$ where $Q = (4\pi/\lambda \sin \theta)$; λ is the neutron wavelength, and 2θ is the scattering angle. When self-assembly occurs, the intensity in the low- Q region will increase with the increase in size and concentration of the particles,¹⁶ and hence we chose to present the

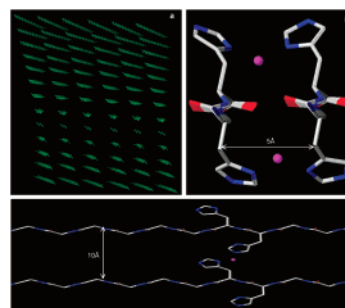


Figure 1. Metal binding sites predicted by the model⁹ of the A β (10–35) fibril. (a) Six-sheet laminated fibril with the backbone atoms shown; (b) potential zinc-binding site, between two β strands within a sheet, perpendicular to the axis of fibril propagation; (c) potential zinc-binding site between two strands of different sheets, viewed down the axis of fibril propagation. Red, oxygen; blue, nitrogen; magenta, metal ion.

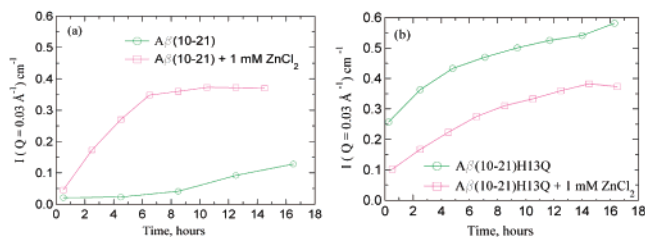


Figure 2. Kinetics of A β (10–21) and A β (10–21)H13Q fibril growth: (a) A β (10–21) and A β (10–21) with ZnCl₂; (b) A β (10–21)H13Q and A β (10–21)H13Q with ZnCl₂. A β (10–21) was dissolved in 100% D₂O and adjusted to 5 mg/mL total peptide concentration, 100 mM NaCl, 10 mM MES, pH 5.6 and either 0 mM or 1 mM ZnCl₂. The A β (10–21)H13Q sample was measured at 1 mg/mL, and for comparison with A β (10–21), the data shown here are normalized for concentration.

SANS data at $Q = 0.03 \text{ \AA}^{-1}$ as a function of aging time. For A β (10–21) in the absence of Zn²⁺, a nucleation phase lasting several hours is followed by a longer growth phase, and in the presence of Zn²⁺, $[\text{Zn}^{2+}]/[\text{peptide}] = 0.3$, a nucleation phase was undetectable, and growth appeared to reach a plateau in 6 h (Figure 2a). By performing the experiments under acidic pHs, the formation of amorphous precipitate, resulting from the low solubility of Zn²⁺ and peptide at pH 7–7.4,^{17–20} was avoided.

Replacement of histidine 13 with glutamine gives the peptide A β (10–21)H13Q. As shown in Figure 2b, even with the higher relative $[\text{Zn}^{2+}]/[\text{peptide}]$ ratio of 1.5, fibril growth is independent of Zn²⁺. The reduced solubility of the H13Q peptide and its increased propensity toward amyloid formation significantly shortened the nucleation phase so as to be undetected by SANS. Consequently, one possible concern is that any further effect of Zn²⁺ may not be resolved. However, following the kinetics at lower

* To whom correspondence may be sent. E-mail: dlynn2@emory.edu, thiyaga@anl.gov.

[†] Emory University.

^{||} University of Chicago.

[‡] Argonne National Laboratory.

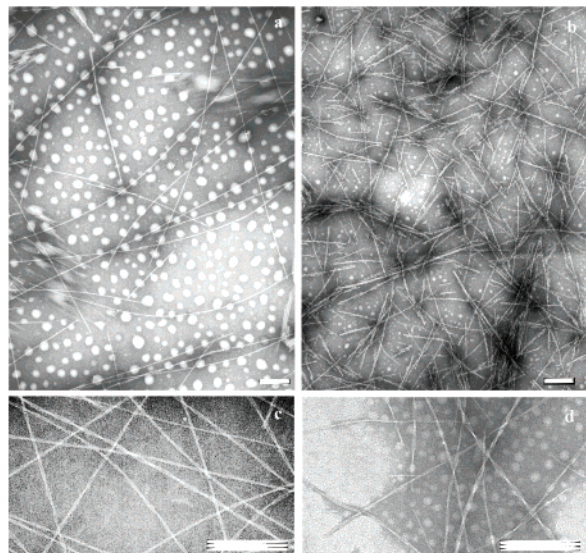


Figure 3. Electron micrograph of fibrils formed by: (a) $A\beta(10-21)$; (b) $A\beta(10-21)$ with 1 mM $ZnCl_2$; (c) $A\beta(10-21)H13Q$; 3d, $A\beta(10-21)H13Q$ with 1 mM $ZnCl_2$. Peptide was dissolved in H_2O and adjusted to 2 mg/mL total peptide concentration, 100 mM NaCl, 10 mM MES, pH 5.4 and either 0 mM or 1 mM $ZnCl_2$. Two-week-old samples, scale bar 200 nm.

concentrations, via HPLC-detected reduction in the concentration of free peptide, did reveal a lag phase that was not affected by varying $[Zn^{2+}]$ (data not shown). Therefore, H13 is required for the observed Zn^{2+} effect.

Previously, the pH dependence of $A\beta(10-35)$ fibrilization was attributed to the $(i, i + 2)$ intra-strand salt-bridge between E11 and H13.⁸ The mutant $A\beta(10-21)E11N$ was prepared, and this peptide also was found to have an increased propensity toward amyloid formation. However, the lag phase in the presence of Zn^{2+} was reduced to the same extent as in $A\beta(10-21)$ (data not shown). Therefore, E11 is not required for the observed Zn^{2+} effect.

The particles being formed were observed directly by transmission electron microscopy (TEM). The lower pH did indeed ensure homogeneous fibril formation; $A\beta(10-21)$ forms long thin fibrils, $35 \pm 5 \text{ \AA}$ in diameter, as well as long twisted pairs with a helical period of 700–1600 \AA (Figure 3a). In the presence of Zn^{2+} , $[Zn^{2+}]/[\text{peptide}] = 0.30, 0.50, \text{ or } 1.5$, the micrographs were strikingly different, and contained a larger number of significantly shorter fibrils (Figure 3b). Fibril width did not appear to be affected by Zn^{2+} either in the TEM images or by SANS. This observation is the expected consequence of nucleation dependent growth when the ratio of nuclei to total peptide concentration increases. Thus, it appears that the presence of Zn^{2+} increases the number or stability of the nuclei. In contrast, the electron micrographs of $A\beta(10-21)$ -H13Q show identical morphologies in the presence and absence of Zn^{2+} (Figure 3c/d), both of which are comparable with those formed by $A\beta(10-21)$ in the absence of Zn^{2+} . Even though amyloid propensity of the H13Q peptide is higher, if the relative rates of initiation and propagation are unaltered, the morphology is expected to be similar. Therefore, Zn^{2+} -binding to $A\beta(10-21)$ must change the rate of nucleation relative to the rate of propagation to explain the observed difference in morphology.

The usefulness of Zn^{2+} in pre-organizing the amyloid nucleus, as demonstrated in this work, has several significant implications. First, most broadly speaking, this work suggests that it is possible to find conditions that differentially alter nucleation and propagation rates and hence opens the possibility of better resolving the precise mechanism of amyloid self-assembly. Second, and more specifically, the data imply the importance of inter-sheet contacts in

amyloid nucleation. As indicated earlier, previous cross-linking analyses have suggested that the laminated β -sheets within the fibril are themselves parallel. The H13Q mutant is therefore predicted to eliminate the possibility of inter-sheet metal binding, while preserving the possibility of intra-sheet metal binding involving the aligned H14 residues. The metal-independence of the H13Q peptide aggregation therefore tends to confirm this structural view of the assembled fibril, and suggests that the increase in nucleation rate in $A\beta(10-21)$ in the presence of Zn^{2+} is due to inter-sheet interactions. Third, the data presented here relate to the epidemiological and biochemical studies carried out by others, correlating metal exposure with the onset of Alzheimer's disease, and offer explanations for the effects which have been described.^{17,20-22} In particular, the results here are consistent with Bush's finding^{18,19} that the mouse $A\beta$ sequence, which contains an H13R mutation, is more tolerant of metal exposure than the human sequence, and relate to the continuing discussion of methods to control amyloid deposition in this context. Finally, and from an entirely different perspective, the occurrence of metals within an organized macromolecular nucleus, such as in the $A\beta$ fibril, raises the possibility of adapting this scaffold for novel materials applications.

Acknowledgment. We thank NIH RR12723, Emory University, the Integrated Microscopy and Microanalytical Facility, and a Grant (No. 99-8327) to D.G.L. and P.T. from The Packard Foundation Interdisciplinary Science Program for financial support.² This work benefited from facilities in the IPNS, as funded by the U.S. DOE, BES under contract W-31-109-ENG-38 to the University of Chicago. We thank D. Wozniak for his assistance in SANS experiments.

References

- Jarrett, J. T.; Lansbury, P. T., Jr. *Cell* **1993**, *73*, 1055–1058.
- Tomski, S. J.; Murphy, R. M. *Arch. Biochem. Biophys.* **1992**, *294*, 630–638.
- Padrick, S. B.; Miranker, A. D. *Biochemistry* **2002**, *41*, 4694–4703.
- Jarrett, J. T.; Lansbury, P. T., Jr. *Biochemistry* **1992**, *31*, 12345–12352.
- Jarrett, D. Y.; Berger, E. P.; Lansbury, P. T., Jr. *Biochemistry* **1993**, *32*, 4693–4697.
- Elser, W. P.; Stimson, E. R.; Ghilardi, J. R.; Vinters, H. V.; Lee, J. P.; Mantyh, P. W.; Maggio, J. E. *Biochemistry* **1996**, *35*, 749–757.
- Teplow, D. B. *Int. J. Exp. Clin. Invest.* **1998**, *5*, 121–142.
- Burkoth, T. S.; Benzinger, T. L. S.; Jones, D. N. M.; Hallenga, K.; Meredith, S. C.; Lynn, D. G. *J. Am. Chem. Soc.* **1998**, *120*, 7655–7656.
- Burkoth, T. S.; Benzinger, T. L. S.; Urban, V.; Morgan, D. M.; Gregory, D. M.; Thiagarajan, P.; Botto, R. E.; Meredith, S. C.; Lynn, D. G. *J. Am. Chem. Soc.* **2000**, *122*, 7883–7889.
- Benzinger, T. L.; Braddock, D. T.; Dominguez, S. R.; Burkoth, T. S.; Miller-Auer, H.; Subramanian, R. M.; Fless, G. M.; Jones, D. N.; Lynn, D. G.; Meredith, S. C. *Biochemistry* **1998**, *37*, 13222–13229.
- Benzinger, T. L. S.; Gregory, D. M.; Burkoth, T. S.; Miller-Auer, H.; Lynn, D. G.; Botto, R. E.; Meredith, S. C. *Proc. Natl. Acad. Sci. U.S.A.* **1998**, *95*, 12407–12412.
- Benzinger, T. L. S.; Gregory, D. M.; Burkoth, T. S.; Miller-Auer, H.; Lynn, D. G.; Botto, R. E.; Meredith, S. C. *Biochemistry* **2000**, *39*, 3491–3499.
- Miura, T.; Suzuki, K.; Kohata, N.; Takeuchi, H. *Biochemistry* **2000**, *39*, 7024–7031.
- Curtain, C. C.; Ali, F.; Volitakis, I.; Cherny, R. A.; Norton, R. S.; Beyreuther, K.; Barrow, C. J.; Masters, C. L.; Bush, A. I.; Barnham, K. J. *J. Biol. Chem.* **2001**, *276*, 20466–20473.
- Klunk, W. E.; Pettegrew, J. W.; Abraham, D. J. *J. Histochem. Cytochem.* **1989**, *37*, 1273–1281.
- Thiagarajan, P.; Burkoth, T. S.; Urban, V.; Seifert, S.; Benzinger, T. L. S.; Morgan, D. M.; Gordon, D.; Meredith, S. C.; Lynn, D. G. *J. Appl. Crystallogr.* **2000**, *33*, 535–539.
- Atwood, C. S.; Moir, R. D.; Huang, X.; Scarpa, R. C.; Bacarra, N. M. E.; Romano, D. M.; Hartshorn, M. A.; Tanzi, R. E.; Bush, A. I. *J. Biol. Chem.* **1998**, *273*, 12817–12826.
- Bush, A. I.; Pettingell, W. H.; Multhaup, G.; Paradis, M. D.; Vonsattel, J. P.; Gusella, J. F.; Beyreuther, K.; Masters, C. L.; Tanzi, R. E. *Science* **1994**, *265*, 1464–7.
- Bush, A. I.; Pettingell, W. H., Jr.; Paradis, M. D.; Tanzi, R. E. *J. Biol. Chem.* **1994**, *269*, 12152–12158.
- Yang, D. S.; McLaurin, J.; Qin, K.; Westaway, D.; Fraser, P. E. *Eur. J. Biochem.* **2000**, *267*, 6692–6698.
- Fraser, P. E.; McLachlan, D. R.; Surewicz, W. K.; Mizzen, C. A.; Snow, A. D.; Nguyen, J. T.; Kirschner, D. A. *J. Mol. Biol.* **1994**, *244*, 64–73.
- McLaurin, J.; Fraser, P. E. *Eur. J. Biochem.* **2000**, *267*, 6353–6361.

JA0273086